Waste and Biomass Valorization (2020) 11:1143–1157
https://doi.org/10.1007/s12649-018-0405-8

ORIGINAL PAPER

Optimization of Fe and Mn Removal from Coal Acid Mine Drainage (AMD) with Waste Biomaterials: Statistical Modeling and Kinetic Study

Dámaris Núñez-Gómez[1] · Flávio Rubens Lapolli[1] · Maria Elisa Nagel-Hassemer[1] · María Ángeles Lobo-Recio[1,2]

Received: 14 October 2017 / Accepted: 14 July 2018 / Published online: 27 July 2018

Abstract

The main characteristics of coal acid mine drainage (AMD) are a low pH and high concentrations of sulfate and different metallic ions. Response surface methodology using the central composite rotatable design (CCRD) model was used to optimize the parameters for AMD remediation with aquaculture farming waste [shrimp shell (SS) and mussel byssus (MB)]. SS was chosen due to its high chitin (a metal sorbent) and calcium carbonate (an acidity neutralizing agent) content, and MB because of its potential synergistic effect for the treatment. The coefficient of determination and standard error results from the analysis of variance have shown the model to be adequate. The predicted values were in good agreement with the experimental values. The best experimental conditions established from the statistical study were 136 rpm, 11.46 g L^{-1} SS and 71.6 g L^{-1} MB. CCRD can efficiently be applied for modeling the AMD remediation with biomaterials and is an economical way of obtaining the maximum amount of information in a short period of time with the fewest number of experiments. Additionally, five kinetic models, i.e., pseudo-first-order, pseudo-second-order, intraparticle diffusion, Bangham and Elovich equation, were tested to investigate the adsorption mechanisms. The kinetic studies revealed that a 200 min contact time is sufficient to transform AMD into water suitable for non-potable reuse. The pseudo-second-order model provided the best fitting of the experimental data, indicating a chemical adsorption mechanism. This research shows the suitability of the proposed treatment, and the information is valuable for designing a low-cost remediation process for AMD.

Graphical Abstract

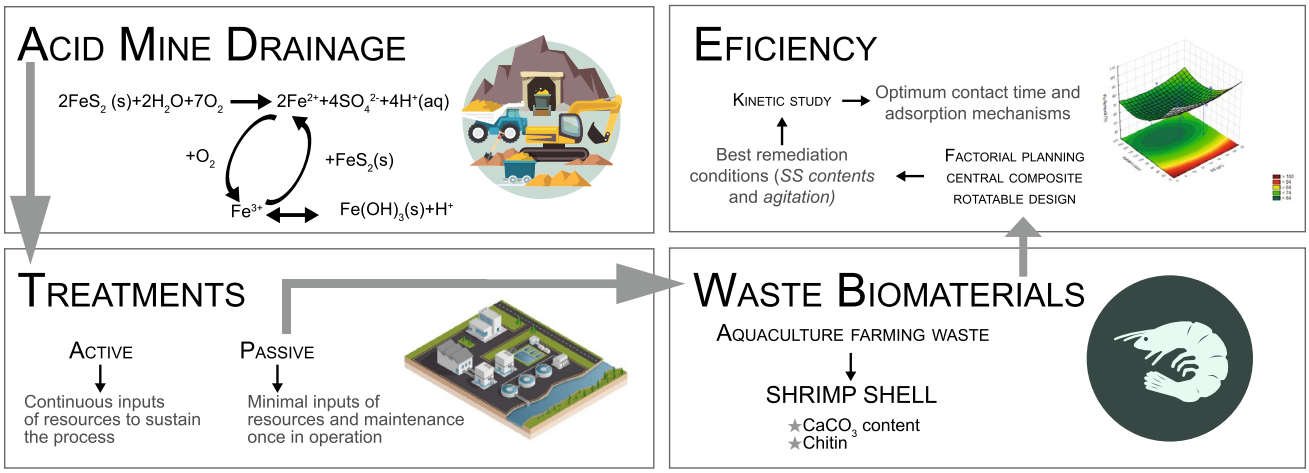

Electronic supplementary material The online version of this article (https://doi.org/10.1007/s12649-018-0405-8) contains supplementary material, which is available to authorized users.

Extended author information available on the last page of the article

Keywords Acid mine drainage (AMD) · Biomaterials · Chitin · Factorial approach · Sorption · Kinetics models

Statement of Novelty

The research goal is to transform acid mine drainage (AMD), an extremely toxic effluent from coal mining, into water suitable for non-potable reuse. With the aim of removing the acidity, iron and manganese, AMD was treated with shrimp shell (SS), a waste from the fish processing industry. SS contains chitin, a metal sorbent, and calcium carbonate, an acidity neutralizing agent. A statistical planning method, the central composite rotatable design (CCRD), was used to determine the optimal agitation rate and relative SS amount. CCRD allowed the best treatment conditions to be established with a low number of assays compared to that required with a conventional method of varying one parameter at a time while holding the others constant. The sustainable nature of this innovative and low-cost technology is notable.

Introduction

Mining practices have caused serious environmental changes over the last century and have made it virtually impossible to maintain aquatic life in affected water bodies. Mines are associated with important environmental problems, such as hindered plant growth and siltation of rivers close to mining activity, all around the world [1–4] and specifically in the study area in Santa Catarina State in southern Brazil [5, 6].

Coal extraction, processing and use generate highly toxic effluents due to the degree of acidity (pH < 4.0), significant metal ion concentrations (Fe, Al, Mn, Cu, Zn, Pb and others) and high sulfate levels. These effluents, known as acid mine drainage (AMD), cause serious environmental problems and can damage ecosystems and human health [7]. Heavy metals are highly harmful because of their non-biodegradable nature, long biological half-lives and potential for toxicity and accumulation in different body parts [8–10].

AMD is generated from chemical and biological processes in which sulfidic minerals, such as pyrite (FeS_2), are oxidized to sulfates with the formation of metallic hydroxides (Eq. 1) [11, 12]. The amount and toxicity of the generated AMD depends on several factors such as the mineralogy of the rock material, surface area, crystallography, temperature, oxygen concentration, and amount of water contacting the material [13]. Remediation of abandoned mining sites is challenging due to the continuous generation of toxic AMD, remote locations of many sites, and extreme mountain weather conditions often present at the contaminated areas.

$$4FeS_2\,(s) + 15O_2 + 14H_2O \rightarrow 4Fe(OH)_3\,(s) + 8SO_4^{2-} + 16H^+ \quad (1)$$

Currently, there are two main approaches for AMD remediation: active and passive treatments. Active treatments require continuous resource input to sustain the process (e.g., water treatment plants and chemical precipitation systems), whereas passive treatments (e.g., constructed wetlands, biochemical reactors, and permeable reactive barriers) require minimal resource input and maintenance once in operation [12, 13]. Both types of treatments use either sorption or another form of chemical/biological treatment to reduce the concentration of metal ions and associated toxicity in AMD.

Due to increasingly limited water resources, innovative technologies can offer a plausible solution to the environmental threats created by closed mines. Traditional water treatments are modeled after wastewater treatment plants, which are machine-intensive and chemical-dependent processes that require continuous operation and maintenance staff. The innovative technology that will be discussed in this paper is largely based on passive treatment systems, has minimal operations and maintenance costs and requires few chemical applications and few, if any, mechanical devices [14].

Biosorption is currently considered a promising technique for heavy metal removal. Biosorption is the process of removing compounds, metal ions or other materials using a sorbent with a biological origin by means of the attractive forces between the removed material and the biosorbent on a cellular structure [7, 15]. Biosorption involves physical and chemical mechanisms such as: physical adsorption, ion exchange, complexation, precipitation, coprecipitation and transport across a cell membrane.

Biosorption by biological materials for removing heavy metals has drawn more and more attention, largely due to the unique properties of these biomaterials, such as environmentally friendly characteristics, low cost, effectiveness at low metal ion concentrations and ease reuse. In recent years, the use of chitinous materials as biosorbents and organic substrates has gained prominence. Chitin $(C_8H_{13}O_5N)_n$ (Fig. 1) has attracted particular consideration because of its capability to chemically or physically adsorb various heavy metal ions [16–19]. The nitrogen in the amino group of the chitin molecule acts as an electron donor and is presumably responsible for selective chelation with metal ions [20, 21]. Chitin, i.e., poly-β-(1,4)-*N*-acetyl-D-glucosamine (Fig. 1), is the most common polysaccharide after cellulose found in nature and can be extracted from crustacean shells, such as shrimp shells [22–25].

Hydric resources in southern Brazil are strongly impacted by coal mine effluents. Most rivers in the coal basin of the Santa Catarina State are contaminated by AMD, rendering the waters unusable. One of the objectives of this research group

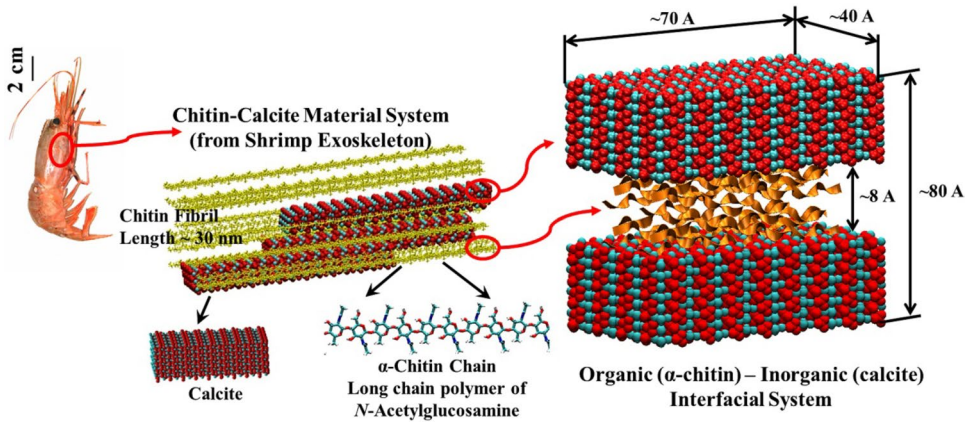

Fig. 1 General exoskeleton structure of shrimp shells [26]

is to transform coal AMD into water that is adequate for non-potable reuse, especially considering the need for preserving limited, high-quality water sources in this region for potable use. Shrimp shell (SS) and mussel byssus (MB) were selected as the AMD treatment agents due to their negligible toxicity and low cost. They are very abundant as refuse in Santa Catarina State without economic value. SS contain high chitin, which is a metal biosorbent, and calcium carbonate, an acidity neutralization agent, contents (Fig. 1). Mussel byssus was chosen to investigate its potential synergic effect on the treatment effectiveness by comparing the results of the treatment with SS alone and with SS and MB. Preliminary studies demonstrated that SS is a better AMD and mine impacted water (MIW) treatment agent than processed chitin [27].

It was hypothesized that SS can serve as a remediation agent at rates competitive with those of other substrates. Since SSs are a waste-product from the seafood industry, the use provides a two-fold benefit: (a) reducing concerns related to waste material disposal and degradation and (b) reducing the overall cost of AMD remediation technologies.

The aim of the research study reported herein was to find the best conditions for an alternative and low-cost solution to the coal AMD problem by producing a neutral pH and metal-free effluent. The specific objective was to apply statistical factorial planning like a central composite rotatable design (CCRD) model to study the best remediation conditions. In addition, a kinetic study was used to investigate the optimum contact time for the sorbent/AMD and the adsorption mechanisms to evaluate the SS efficiency as an alternative to lime, a low-cost biomaterial, for AMD remediation to obtain a neutral pH and metal-free effluent.

Materials and Methods

Biomaterials

SS *in natura* flakes were used as the acidity and metal-ion removal agent. The SS (without the head) was meticulously washed with water to eliminate the remains of organic matter and other coarse materials; subsequently, the shells were dried in an oven for 72 h at 100 °C for the first 48 h and at 50 °C for the last 24 h. After this process, the SS were pulverized in a blender and sieved to promote a greater homogeneity and contact surface area. To prevent moisture absorption, they were kept in a glass desiccator until use [27, 28].

Dry mussel byssus (MB) was used as a low-cost support material for SS to predict the operation of a continuous-flow remediation system in future research. MB was obtained from *Blocaus Pré Fabricados Ltda*, a Brazilian company specializing in the manufacturing of concrete blocks through the use of mariculture residues (oysters and mussels). MB was washed with pressurized water and sun-dried for a minimum of 14 days.

Acid Mine Drainage (AMD) Samples

The AMD samples for the tests were obtained from a 33-year-old inactive coal mine in Urussanga City located within the Carboniferous Santa Catarina Region in the southern Santa Catarina State, Brazil. Samples were

collected at points of easy access in 5 L polypropylene bottles (non-sterile), transported and maintained at a constant temperature of 4 °C, and characterized on the same day as the collection to determine the pH (pH meter ThermoFisher, Scientiphic Orion 3Stars) and metal and metalloid species using an (ICP-MS) inductively coupled plasma mass spectrometer (ICP-MS, Perkin Elmer, Nexlon 300D) following the EPA Method 3005 A [29]. Anions were measured at room temperature using an ion chromatograph (Dionex ICS—1000).

Liquid samples were filtered through a 0.22-µm membrane filter (Sartorius Company) to remove solids and acidified with a concentrated HNO_3 solution to avoid precipitation of metals due to changes in pH [30].

Preliminary Tests

To identify the remediation process and establish the minimum operating parameters, different batch microcosms were prepared to analyze the influence of the pH, relative amount of substratum/water volume (0 and 10 g L^{-1} for MB; 10, 14 and 18 g L^{-1} for SS), and synergy/behavior of the biomaterials in the remediation of AMD [27].

Batch microcosms were maintained at a constant temperature (25 ± 2 °C) and agitated (150 rpm) for 24 h. Control experiments without biopolymers were also carried out. The metals ions were monitored during the experiment by atomic absorption spectrophotometry (AAS) analyses [31] in a Hitachi Z-8230 model spectrophotometer. The pH was monitored during the whole process.

Central Composite Rotatable Design (CCRD)

Factorial design was employed to reduce the total number of experiments needed to determine the best overall optimization of the system. The design determines which factors have important effects on a response and how the effect of one factor varies with the level of the other factors. The determination of factor interactions can only be determined using statistical designs of experiments since the system optimization cannot be performed by varying one factor at a time while fixing the other factors [32].

For this study, a central composite rotatable design (CCRD) was created with three factorial variables (2^3) and applied to optimize the remediation process and identify the ideal parameters for the experiment. Agitation and the SS and MB contents were chosen as the independent variables, and the final concentrations of the metal species, Fe and Mn, were the dependent variables (responses). The contact time was not considered an independent variable because the ideal time was identified experimentally in kinetic experiments. Subsequently, the ideal amounts of SS and MB and agitation speed were determined in this factorial experimental planning.

The factor scores (+1 and −1) that indicate the minimum and maximum levels to test for each of the variables, the center point (0) and axial points (+1.68 and −1.68), were calculated by Eq. 2, where α is the axial distance from the point and n is the number of independent variables (n = 3) used in the experiment. The experiments consisted of eight assays (−1 and +1) plus three center points and six axial points (−1.68 and +1.68), resulting in an orthogonal distribution, and a total of 17 experiments were carried out by using the rotatable central composite design, as shown in Table 1. Based on the preliminary experimental results, the levels chosen for the independent variables, agitation (X_1), MB (X_2) and SS (X_3) are listed in Table 2. The experimental data were analyzed using statistical methods appropriate for the experimental design used.

$$\alpha = (2^n)^{\frac{1}{4}} \quad (2)$$

The experiments were performed in a thermostatic bath (Dubnoff 252), and when more precise agitation was necessary [axial points −1.68α (16 rpm) and +1.68α (184 rpm)], magnetic agitation was used (mark Dist). In all cases, 100 mL of the liquid samples was placed in non-sterile, polypropylene Erlenmeyer flasks with a 250-mL total capacity, and the flasks were capped with plastic wrap to prevent the entry of environmental dirt and/or water from the thermostatic bath.

All experiments were performed with a 24 h contact time, AMD/biopolymer and a controlled temperature (25 °C ± 2). For sample filtration, cellulose acetate membranes with a

Table 1 Matrix for CCRD

Run	X_1	X_2	X_3
1	0	0	0
2	0	0	+1.68
3	−1	+1	+1
4	−1.68	0	0
5	+1	−1	+1
6	+1	+1	−1
7	0	0	0
8	−1	−1	−1
9	+1	−1	−1
10	+1	+1	+1
11	0	+1.68	0
12	−1	−1	+1
13	−1	+1	−1
14	+1.68	0	0
15	0	0	0
16	0	0	−1.68
17	0	−1.68	0

Table 2 Independent variables and their levels for CCRD

Variable	Symbol	−1.68α	−1	0	+1	+1.68α
Agitation (rpm)	X_1	16	50	100	150	184
Mussel byssus (g L^{-1})	X_2	0.72	2.0	6.0	10.0	13.26
Shrimp shell (g L^{-1})	X_3	7.28	10.0	14.0	18.0	20.72

0.45-µm porosity were employed. To monitor the possible changes in the intrinsic conditions, a blank was tested (no biopolymer liquid sample).

The residual heavy metal ion concentrations were determined by atomic absorption spectrophotometry (AAS) as in the preliminary tests [31]. The pH was also monitored during the entire process.

The mathematical models were evaluated for each response by means of multiple linear regression analyses. The significant terms in the model were found by analysis of variance (ANOVA) for each response with STATISTICA 13.1 *StatSoft* software. The value of the model is that it identifies statistically different significant factors, allows a confidence performance prediction by interpolation over a range of data, and facilitates the construction of response surface (3D and 2D) graphs, which help to understand the process under investigation.

Adsorption Kinetics in Batch Experiments

Batch adsorption tests were performed to determine the adsorption kinetics. For this purpose, an orbital shaker thermostatic bath (Dubnoff 252) and a set of 20 non-sterile polypropylene Erlenmeyer flasks were used. The Erlenmeyer flasks were filled with 200 mL of AMD and 11.46 g of SS for a total contact time of 4320 min at a constant temperature (25 ± 2 °C) using an agitation speed of 105 rpm. In all cases, the Erlenmeyer flasks were capped with plastic wrap. The SS amount and agitation speed were previously determined using factorial experimental planning.

To monitor the adsorption process, each Erlenmeyer flask was opened at different times, and samples were taken and analyzed to determine the removal of the metal ions. A parallel control experiment without SS was also carried out. The pH of the solution was measured during the process. The samples were filtered (0.22 µm), and the residual metallic ion content was determined by atomic absorption spectroscopy (AAS). The percentage of Fe and Mn removal (% removal) was calculated using Eq. 3. To evaluate the kinetic mechanism of the adsorption process, pseudo-first-order, pseudo-second-order, intraparticle diffusion, Elovich and Bangham models were used to fit the experimental data.

$$\%\ \text{Removal} = \frac{C_0 - C_t}{C_0} \times 100 \tag{3}$$

where C_0 is the initial metal ion concentration, and C_t is the metal ion concentration (mg L^{-1}) at time *t*.

Sorption Kinetic Models

To analyze the predominant sorption process mechanism, such as chemical reaction, diffusion control and mass transfer, five kinetic models were used to test the experimental data.

Pseudo-First-Order Equation The pseudo-first-order equation in its linear form is expressed in Eq. (4) [33].

$$\log(q_1 - q_t) = \log q_1 - \frac{k_1}{2.303} t \tag{4}$$

where q_1 and q_t refer to the metal amounts sorbed at equilibrium and at time t (mg g^{-1}), respectively, and k_1 is the rate constant of pseudo-first-order sorption (L min^{-1}).

Pseudo-Second-Order Equation The pseudo-second-order chemisorption kinetic rate equation in a linear form is expressed in Eq. (5) [34].

$$\frac{t}{q_t} = \frac{1}{k_2 q_2^2} = \frac{1}{q_2} t \tag{5}$$

where q_2 is the amount of metal ion sorbed at equilibrium (mg g^{-1}), and k_2 is the equilibrium rate constant of pseudo-second-order sorption (g mg^{-1} min^{-1}). This model also can be used to obtain the value of an important parameter, the initial sorption rate [h, (mg g^{-1} min^{-1})], as indicated in Eq. 6.

$$h = k_2 q_2^2 \tag{6}$$

Intraparticle Diffusion Equation This is a fractional approach to equilibrium changes according to the function $(Dt/r^2)^{1/2}$, where *r* is the particle radius and D the diffusivity of a solute within the particle [35]. The rate parameter (k_{int}) for intraparticle diffusion can be defined as Eq. 7:

$$q_t = k_{\text{int}}^{\frac{1}{2}} \tag{7}$$

where k_{int} is the intraparticle diffusion rate constant (mg g^{-1} $min^{1/2}$).

Elovich Equation The Elovich equation is given as Eq. 8 [36]:

$$q_t = \frac{1}{\beta}\ln(\alpha\beta) + \frac{1}{\beta}\ln\ t \tag{8}$$

where α is the initial sorption rate (mg g^{-1} min^{-1}), and the parameter β is related to the extent of surface coverage and activation energy for chemisorption (g mg^{-1}).

Bangham Equation The Bangham equation was used to evaluate whether the adsorption was pore-diffusion controlled [37].

$$\log\left\{\left[\frac{C_i}{C_i - Mq_t}\right]\right\} = \log\left[\frac{K_b M}{2.303V}\right] + \propto \log t \tag{9}$$

where C_i is the initial metal ion concentration (mg L^{-1}), V is the volume of the solution (mL), M is the mass of the adsorbent (g L^{-1}), q_t is the amount of adsorbate retained at time t, and α (< 1) and K_b are constants that can be obtained from slope and intercept, respectively.

Results and Discussions

The pH of the raw AMD was 3.04. The total metal concentrations found in the raw AMD are reported in Table 3, and they are within the ranges found in the literature [38–40]. In this case, only the pH, Fe_{total} and Mn_{total} concentrations were monitored because other pollutants were below the Brazilian legal limits for effluent discharge [41]. Henceforth, Fe_{total} and Mn_{total} will be used to indicate the Fe and Mn concentrations, respectively.

Table 3 Initial characterization of the AMD used in the tests

Variable	Unit	Value	CONAMA 430/2011[a]	CONAMA 357/2005[b]
pH	–	3.04	5–9	6–9
Sulfate	mg L^{-1}	3630.8		250
Fe_{total}	mg L^{-1}	83.24	15.0	5.0
Mn_{total}	mg L^{-1}	5.94	1.0	0.5
Al	mg L^{-1}	0.020		0.2
Nd	mg L^{-1}	27.67×10^{-3}		
Cd	mg L^{-1}	0.001	0.2	0.01
K	mg L^{-1}	8.880		
Co	mg L^{-1}	0.078		0.2
Cu	mg L^{-1}	0.012	1.0	0.013
Ni	mg L^{-1}	71.04×10^{-3}	2.0	0.025

[a]Brazilian legal limits for effluent discharge

[b]Brazilian legal limits for reuse of water for non-potable secondary uses

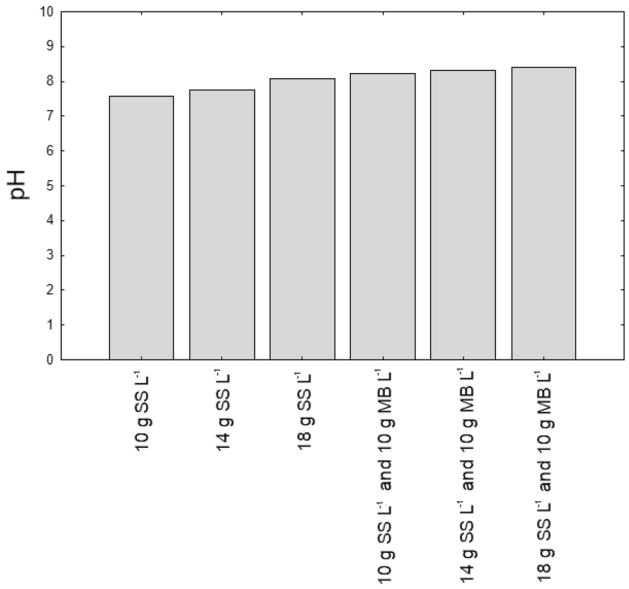

Fig. 2 Preliminary results for pH

Preliminary Tests

The addition of biomaterials to the AMD samples caused a rapid increase in the pH in all the microcosms. In bottles with SS and MB, the pH increased from pH 3.04 to 8.22 (with 10 g L^{-1} each of the biomaterials) and to pH 8.42 with 18 g L^{-1} of SS and 10 g L^{-1} of MB, while in the other microcosms, the pH reached 7 (Fig. 2). The increase in the pH was higher in the batch tests with a higher SS content (18 g L^{-1}) than those with other SS contents (10 and 14 g L^{-1}), which is possibly due to the larger amount of calcium carbonate. This indicated the suitability of SS as a low-cost neutralizing

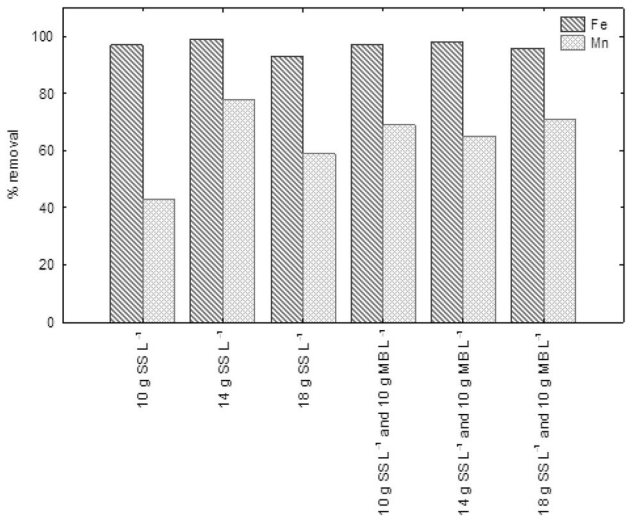

Fig. 3 Preliminary metal removal results

agent and its influence on the process of AMD remediation and neutralization.

Metallic ion removal was extremely dependent on the pH. For both metals, the best results were observed with the combination biomaterial microcosms. The best removal rates for Fe (96%) and Mn (78%) were obtained with SS and MB (with 18 g L^{-1} SS and 10 g L^{-1} MB) (Fig. 3) due to the combined action of the sorption mechanisms on the biomaterials and precipitation as hydroxides. In the control bottles, the pH and metal concentrations remained unchanged throughout the experiment.

The experiments indicated the synergy of biomaterials in the overall treatment effectiveness in terms of the metal ion removal. The SO_4^{2-} content, as expected, almost did not change after the treatment (3630.8 mg L^{-1}), which indicated that under the conditions tested, the biomaterials (SS and MB) were not adequate for the removal of this contaminant and agreed with previous research results [27, 28]. Therefore, the next experiments were carried out with SS and MB simultaneously.

Factorial Design

For Fe, all conditions tested had a high removal percentage (between 70 and 90%) of species, and for Mn, 41% of the tests showed a high removal percentage (> 70%), which confirmed the validation of the factorial design for AMD remediation through treatment with a combination of SS and MB (Table 4).

Table 4 Factorial design (2^3) results for AMD remediation by treatment with SS and MB

Run	Independent variables			Dependent variables (% removal)	
	X_1	X_2	X_3	Fe	Mn
1	0	0	0	96.9	90.0
2	0	0	+1.68	77.9	38.1
3	−1	+1	+1	83.5	40.3
4	−1.68	0	0	84.9	78.0
5	+1	−1	+1	96.9	89.0
6	+1	+1	−1	93.4	73.3
7	0	0	0	85.7	76.3
8	−1	−1	−1	96.1	25.2
9	+1	−1	−1	96.3	39.6
10	+1	+1	+1	75.1	21.8
11	0	+1.68	0	91.8	5.9
12	−1	−1	+1	95.3	44.0
13	−1	+1	−1	80.8	10.3
14	+1.68	0	0	82.8	4.2
15	0	0	0	81.8	95.4
16	0	0	−1.68	72.3	49.9
17	0	−1.68	0	82.6	73.6

Central Composite Rotatable Design (CCRD)

Brasil et al. [42] showed that metallic ion uptake by a biosorbent in a batch system usually depends on several factors, such as the pH, metallic ion concentration, biomaterial content, shaking, and contact time. The optimization of all those variables using a univariate procedure is very complex because a variable or factor is only optimized by varying just one factor at a time and fixing the others. The disadvantage of this univariate procedure is that the best conditions may not be attained because the interactions among all the factors are neglected. It cannot be known if the other fixed variables were kept at other levels, if the results would lead to the same optimization. In addition, the total number of experiments to be carried out in a univariate procedure is much higher than that with a statistical design of experiments [42].

The best performance of a factorial design depends on some knowledge about the system being optimized. The definitions of the factors and levels in the CCRD are presented in Tables 1 and 2.

For the calculated effects to be statistically significant, the p value should be less than 0.05 at a significance level of 95%. Thus, by using this estimation, the variables tested, when considered individually, have different behaviors for each particular species. In this regard, while the removal of Fe (Table 5) showed a single variable, agitation (L), had a significant influence ($p < 0.05$), Mn (Table 6) had three significant variables, the biomaterial contents (SS and MB, both in the quadratic form) and agitation (linear and quadratic forms). A similar performance was observed in other studies [28]. To facilitate viewing in the tables in which

Table 5 Estimated effects on the Fe removal variable

	Coefficient	Effect	SE[a]	t(2)	p value
SS (L)	Q_1	0.85	13.60	0.06	0.95
SS (Q)	Q_{12}	2.85	14.74	0.19	0.85
Agitation (L)[b]	**Q_2**	**66.67**	**14.21**	**4.69**	**0.002**
Agitation (Q)	Q_{22}	8.61	14.74	0.58	0.57
MB (L)	Q_3	− 3.27	14.46	v0.23	0.82
MB (Q)	Q_{32}	− 9.34	17.22	0.60	− 50.06
SS (L) by Agitation (L)	$Q_1 vs Q_2$	1.48	17.76	0.08	0.93
SS (L) by MB (L)	Q_1 vs Q_3	− 11.87	17.76	− 0.67	0.52
Agitation (L) by MB (L)	Q_2 vs Q_3	− 9.41	17.76	− 0.52	0.61

[a]Standard error

[b]Significant variables ($p < 0.05$) are in bold

Table 6 Estimated effects on the Mn removal variable

	Coefficient	Effect	SE[a]	t(2)	p value
SS (L)	Q_1	− 2.99	6.05	− 0.49	0.67
SS (Q)[b]	**Q_{12}**	**− 32.32**	**6.56**	**− 4.92**	**0.03**
Agitation (L)[b]	**Q_2**	**− 28.11**	**6.05**	**− 4.65**	**0.04**
Agitation (Q)[b]	**Q_{22}**	**− 33.60**	**6.56**	**− 5.12**	**0.03**
MB (L)	Q_3	9.37	6.43	1.46	0.28
MB (Q)[b]	**Q_{32}**	**− 37.34**	**7.66**	**− 4.87**	**0.03**
SS (L) by agitation (L)	Q_1 versus Q_2	− 7.62	7.90	− 0.96	0.43
SS (L) by MB (L)	Q_1 versus Q_3	− 17.90	7.90	− 2.26	0.15
Agitation (L) by MB (L)	Q_2 versus Q_3	− 22.09	7.90	− 2.79	0.10

[a]Standard error

[b]Significant variables ($p < 0.05$) are in bold.

the estimated effects are shown, the significant variables ($p < 0.05$) are highlighted.

The positive values of effects mean that an increase in their levels leads to an increase in the metallic ion uptake by the biomaterial; on the other hand, the negative values of the effects lead to a diminution in the response as their levels increase [42].

Then, using the significant variables, analysis of variance (ANOVA) was performed, and for the removal of Fe and Mn (Table 7), $F_{calculated} > F_{tabulated}$. Therefore, the ANOVA analysis regarding the removal of these species showed that the model for Fe and Mn removal is valid at the 95 and 99% confidence intervals, respectively, and no adjustment is needed within the range evaluated, resulting in excellent reproduction in the experimental samples.

The fit of the attained regression model was checked by the coefficient of determination, R^2. The values of R^2 for Fe ($R^2 = 0.88$) and Mn ($R^2 = 0.94$) were close to 1, which indicated a high degree of correlation between the response and the independent variables for the two responses (experimental and predicted values) [43]. The value of the Mn determination coefficient, R^2 (0.94), suggested that approximately 6% of the total variation is not explained by the model. For Fe, the percentage increased to 12%. Since there were replicated center points, the software obtained a lack-of-fit, but the insignificant lack-of-fit test (Mn F value = 13.51 and Fe F value = 2.013) indicated that the model was suitable to represent the experimental data.

As a complement, the validation of the model was also performed by the distribution of residuals graphical observations for each case, i.e., the model-established values versus the experimentally observed values (Fig. 4). The values predicted by the model are represented by a line, while the observed values are represented by points. The experimentally observed values are relatively close to the line with positive and negative variances of approximately the same proportion. Thus, Fig. 4 shows a strong correlation between the predicted and experimental values, which indicates the goodness of fit.

The first goal of the response surface method is to find the optimum response. The second goal is to understand how the response changes in a given direction by adjusting the design variables. In general, the response surface can be visualized graphically. The graph is helpful to see the shape of a response surface. Hence, the function $f(X_1, X_2, X_3)$ can be plotted vs the levels of X_1, X_2 and X_3, as indicated in Fig. 5a–d. The curvatures in the 3D plots arise due to the quadratic dependency on the responses and parameters.

The results indicate that 94–100% of Fe removal was observed with low agitation speeds (0–40 rpm) and was independent of the SS (Fig. 5a) and MB contents (Fig. 5b), which confirmed the relationship and dependence on agitation as a significant variable of the process. High iron removal was also observed with 190–200 rpm agitation speeds and 0–40 g L^{-1} MB (Figs. 5b, 6b). On the other hand, the best result for Mn removal (> 80%) was with high SS (Fig. 5c) and MB contents (Fig. 5d) in the transversal region (between 14 and 18 g L^{-1} SS and 60–80 g L^{-1} MB) and between 100 and 140 rpm, which was in accordance with the factorial design.

Sometimes, it is easier to observe the response surface in 2D graphs. The contour plots can show the contour lines of

Table 7 Analysis of variance for the Fe and Mn removal variables in 2^3 factorial designs

Parameter	Variation source	Seq. SS	df	MS	*F.*		*p*
					Cal	Tab[a]	
Fe removal	Regression	1501.41	9	1501.41	4.10	3.68	< 0.05
	Sediments	4417.96	7	631.13			
	Total	6089.12	16				
Mn removal	Regression	14002.18	9	14002.18	11.29	6.72	< 0.01
	Sediments	8682.51	7	1240.35			
	Total	19400.38	16				

Seq SS sum of square, *df* degree of freedom, *MS* mean square, *F* factor F, *p* probability

[a]Tabulated values [32]

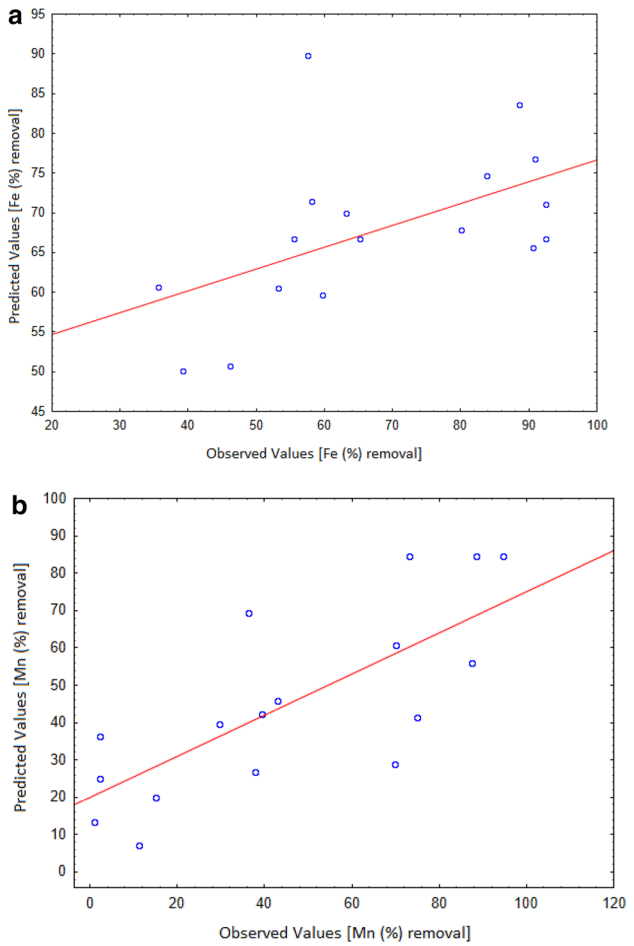

Fig. 4 Residual distributions for **a** Fe (%) removal ($R^2 = 0.88$) and **b** Mn (%) removal ($R^2 = 0.94$)

the independent variables that have the same response value, y. From the response surface contour plots, it is very easy to understand the interactions between two independent variables and to locate their optimum levels. Figure 6 presents the contour plots for metal ion removal (Fe and Mn) for each pair of parameters as the other factors were held constant at their middle level. An elliptical contour plot indicates that the interactions between them are significant. Figure 6a–d show that there were a few interactions among the independent variables since the range of the response surface is wide for each of these parameters.

With these results, it was possible calculate the statistical optimal points with a maximal removal efficiency. A high biomaterial content (> 11.0 g L^{-1} of SS and > 54.0 g L^{-1} of MB) and mechanical agitation in the range of 75–137 rpm were needed for high metal removal (Table 8).

These data show the significant effect of the SS content in the metal ion removal process, which is possibly because the metal species adsorb on the chitin biopolymer and SS increases the liquid sample pH, enhancing the removal of species via precipitation as hydroxides.

Based on the individual optimal values and percentage for the initial metal concentrations considered, STATISTICA 13.1 *StatSoft* software determined that 136 rpm, 11.46 g L^{-1} SS and 71.6 g L^{-1} MB were the best experimental conditions for the highest simultaneous removal efficiency of iron and manganese. The results were in agreement with other work focused on statistical planning for AMD remediation [28], but the specificity of the statistical study, i.e., the choice of the biomaterials and the composition of the effluent, makes it difficult to compare this study with other works.

Adsorption Kinetics in Batch Experiments

Metal sorption kinetics is influenced by the sorption mechanism and the mass transfer steps that govern the transfer of metal ions from the bulk of the solution to the sorption sites on the surface and inside adsorbent particles, i.e., external and intra-particle diffusion. In turn, these mechanisms depend on the physical form of the sorbent (flake size), which was chitin in our case, the intrinsic structure of chitin (purity, crystallinity, and molecular weight), the nature of the metal and the solution, and the process conditions (temperature and pH). Simplified models can be used to test batch experimental data and identify the rate-controlling mechanisms for the adsorption process [44]. In this case, five different models were used to predict the sorption kinetics of Fe and Mn onto SS.

pH Variation

The solution pH plays an important role in the adsorption of metal ions on various adsorbents, and the pH affects both the dissociation degree of the functional groups on the adsorbent surface and the speciation/solubility of metal ions. In this study, the initial pH was 3.04, and at that pH, according to the iron and manganese speciation diagrams [45], Mn is predominantly present in a divalent form and Fe is present as divalent and trivalent free ions. Other species can be involved in chemical processes during sorption on SS.

Figure 7 shows the shift in the pH of the solution caused by the addition of SS. The initial pH increased (from 3.04 to 6.65) in the first 5 min, which was probably due to the calcium carbonate constituent of the SS. A moderate pH increase was observed until 4320 min, and the maximal value of 8.78 was reached. After that time, no further significant pH modifications occurred. This could be because the SS carbonate was completely consumed, and the biomaterial was saturated (Eq. 10).

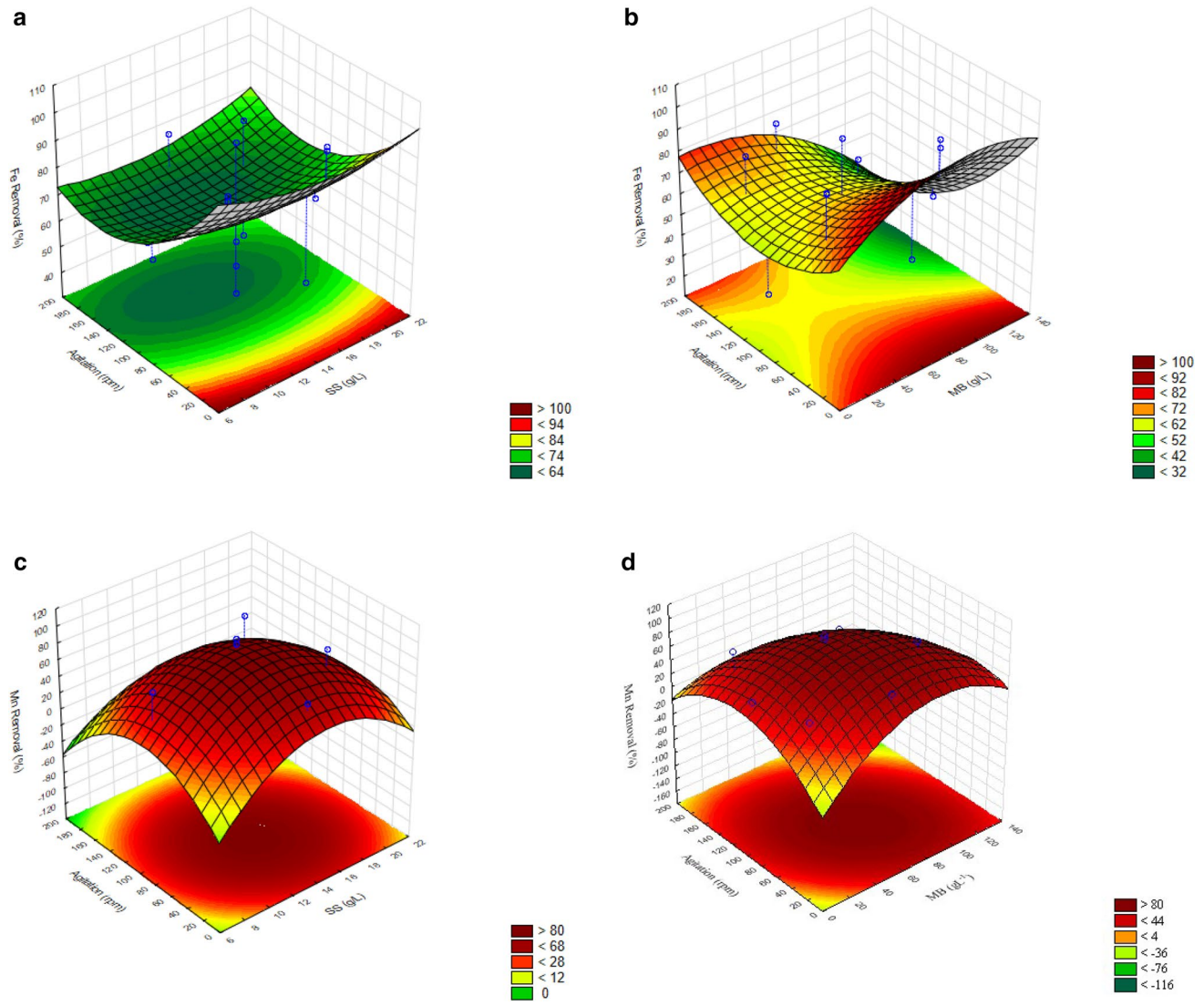

Fig. 5 Contour curve for Fe removal (**a** for SS content and **b** for MB content) and Mn removal (**c** for SS content and **d** for MB content)

$$CaCO_3\ (s) + H_2O \leftrightarrow CaCO_3\ (aq) + H_2O \leftrightarrow Ca^{2+} + HCO_3^- + OH^-; M^{2+} + 2OH^- \rightarrow M(OH)_2\ (s) \quad (10)$$

where M^{2+} represents a divalent metal ion.

Contact Time

The relationship between the contact time and Fe and Mn sorption onto SS was analyzed under the following conditions: 83.24 mg Fe_{total} L^{-1} and 5.94 mg Mn_{total} L^{-1} initial solution concentration, initial pH = 3.04, 11.46 g SS L^{-1} and 71.6 g MB L^{-1} biomaterial content and 136 rpm agitation speed. The results presented in Fig. 8 show the very fast sorption of Fe and Mn in the first 80 min, which was followed by a slower process until approximately 150 min.

At that point, equilibrium was attained for both metals (90% Mn removal and 93% Fe removal). At this time, the residual Fe and Mn concentrations were 5.83 and 0.59 mg L^{-1}, respectively, and these values are below the maximum values allowed by the Brazilian normative for effluent discharge (15.0 and 1.0 mg L^{-1}, respectively) [41]. The fast uptake at the beginning suggested the occurrence of a rapid external mass transfer that involved rapid attachment of the metal ions to the surface of the sorbent with a pH influence. A similar trend was observed for the sorption of ions using a commercial chitin complex [46]. After 200 min of contact time, both the Fe (4.32 mg L^{-1}) and Mn (0.4 mg L^{-1}) residual contents were below the limiting value for water

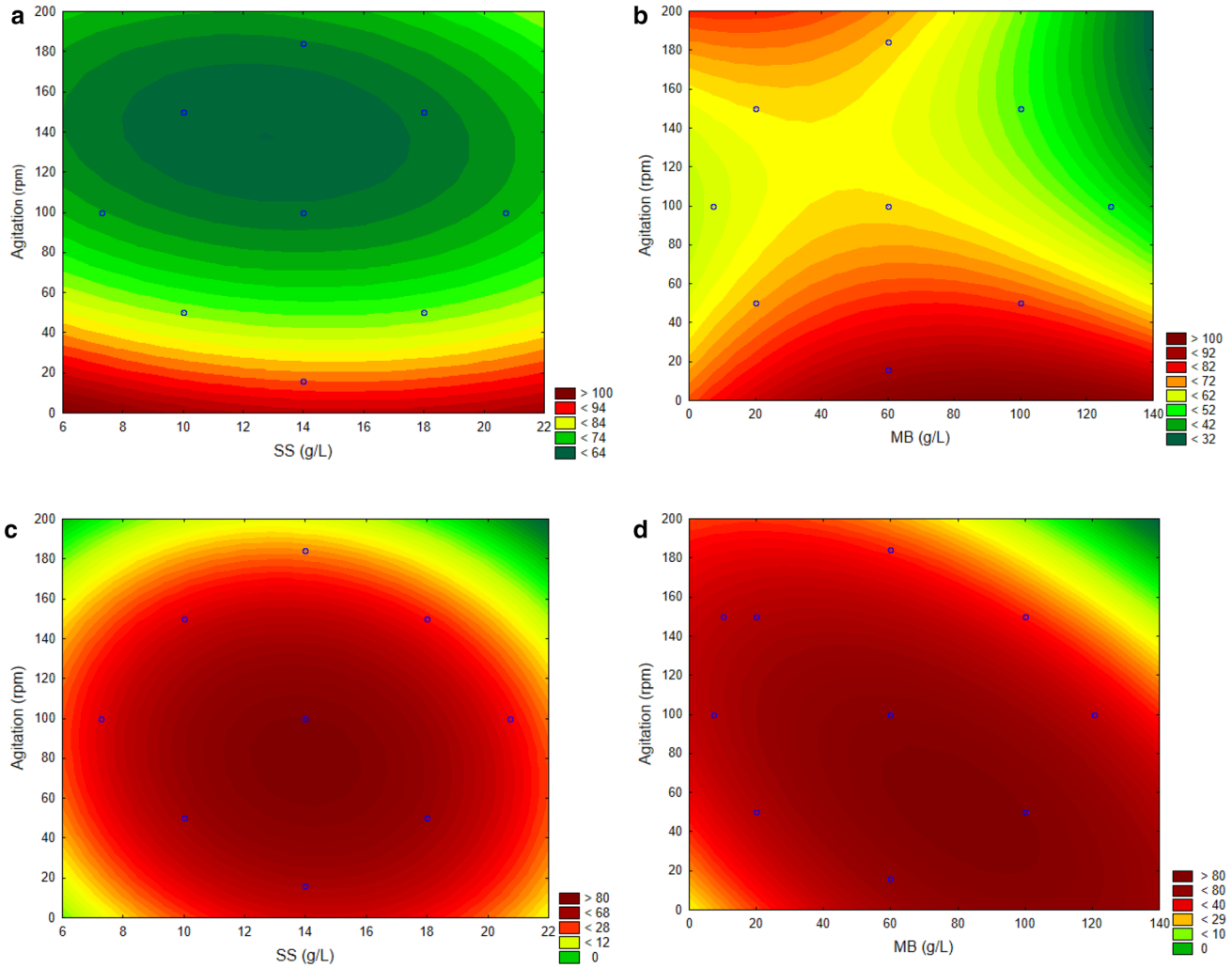

Fig. 6 Response surface for Fe removal (**a** for SS content and **b** for MB content) and Mn removal (**c** for SS content and **d** for MB content)

reuse allowed by the Brazilian normative (Fe, 5.0 mg L^{-1}; Mn, 0.5 mg L^{-1}) [47], which indicated that the treated effluent is suitable for use as non-potable reuse water.

The maximum Fe (100%) and Mn (98%, 0.12 mg L^{-1}) removals from AMD were observed at 3240 and 2880 min, respectively (Fig. 8). In addition to the adsorption mechanism, the elevated pH of the sample (pH > 8) can help remove dissolved metallic ions by precipitation of hydroxides. In the pH range of 7.80–8.76, the removal capacity remains approximately constant. The obtained results show that the pH is an important parameter in the metal ion sorption mechanism [36]. This dependence between the solution pH and biosorption suggested that SS can be developed as a multi-use, low-cost sorption material.

Table 8 Ideal optimal values of maximum efficiency in the Fe and Mn removal processes

Element	Agitation (rpm)	SS (g L^{-1})	MB (g L^{-1})
Fe	137	11.46	54.33
Mn	75	13.73	71.66

Kinetics Models

The sorption kinetic data can provide valuable insight into the reaction pathways and mechanism of a sorption process. To obtain some insight into the kinetics of the removal of Fe and Mn by SS, the experimental data were fitted by five common models, which included the pseudo-first-order model, pseudo-second-order model, intraparticle diffusion model, and Elovich and Bangham equations (Eq. 4–8) (Fig. 1 supplementary material). These models were assessed based on their regression parameters, R^2, to determine if they were applicable to the adsorption

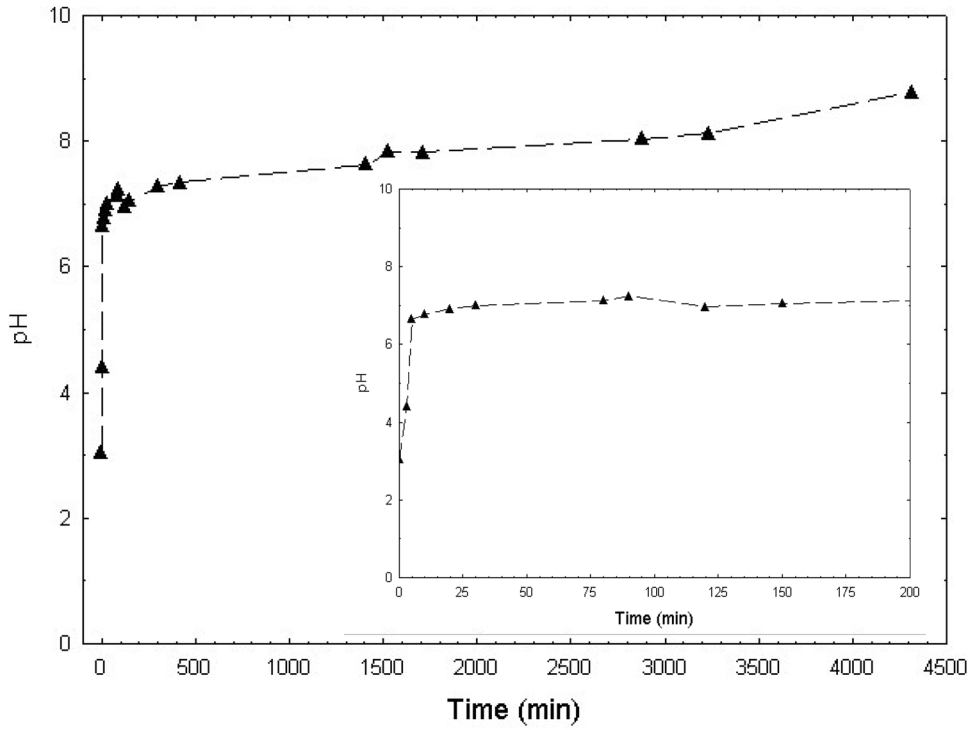

Fig. 7 pH variation as a function of the contact time with an emphasis on the first 200 min

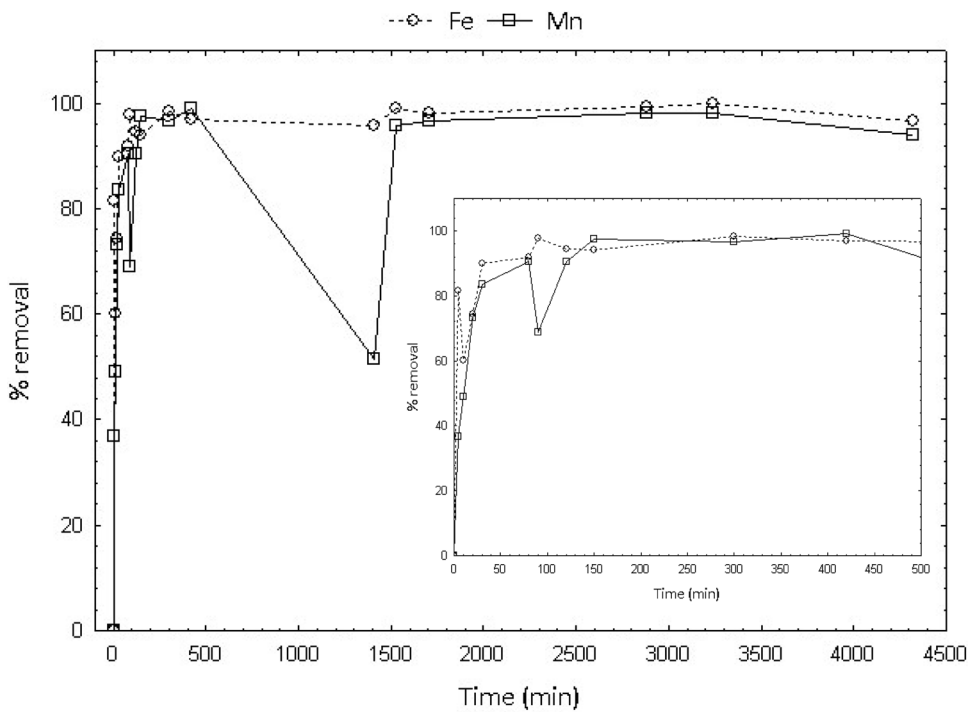

Fig. 8 Metal ion removal (%) onto SS as a function of contact time with an emphasis on the first 500 min

process. The rate constants and correlation coefficients of the kinetics models are shown in Table 9.

For both metal ions, the correlation coefficients were lower than 0.85 for the pseudo-first-order model, intraparticle diffusion, Elovich equation, and Bangham equation, which indicated that these models have a limited applicability for the interpretation of the experimental results. Thus, these kinetics models were not suitable to describe the kinetics of Fe and Mn sorption onto SS.

Moreover, the experimental data for Fe and Mn sorption onto SS were well fit by the pseudo-second-order kinetic model with high correlation coefficients, higher than 0.96,

Table 9 Kinetic parameters for Fe and Mn removal onto SS

	Fe	Mn
Pseudo-first-order		
R^2	0.83	0.61
K_1 (L min^{-1})	0.86	0.03
q_e cal (mg g^{-1})	1.03	0.01
Pseudo-second-order		
R^2	0.99	0.96
K_2 (g mg^{-1} min^{-1})	0.26	0.21
q_e cal (mg g^{-1})	1.38	0.65
h (mg g^{-1} min^{-1})	0.50	91.35×10^{-3}
Intraparticle diffusion		
R^2	0.58	0.75
K_{in} (g mg^{-1} $min^{-1/2}$)	0.07	0.04
Elovich equation		
R^2	0.50	0.83
α (mg g^{-1} min^{-1})	4.12	0.45
β (g mg^{-1})	3.07	2.96
Bangham equation		
R^2	0.55	0.85
K_b (g)	46.85	12.38
α	0.077	0.14

which suggested that the rate limiting step may be chemical sorption or chemisorption involving valence forces through sharing or exchange of electrons between the sorbent and sorbate [48–50]. Similar results were reported for adsorption in dye-chitosan systems [49], the sorption of zinc on solids [51] and the sorption of iron, cobalt, nickel, copper and zinc on solvent-impregnated resins [52, 53].

Consequently, a chemisorption kinetic model, such as the pseudo-second-order model, is likely the most appropriate model for the sorption of Mn and Fe ions onto SS under the tested conditions.

The kinetics of sorption by SS of the Fe and Mn ions dissolved in AMD were fast (K_2 (Fe) = 0.26 g mg^{-1} min^{-1} and K_2 (Mn) = 0.21 g mg^{-1} min^{-1}) when compared with other studies, like remediation of coal acid mine impacted water (MIW) onto SS too (K_2 (Fe) = 0.106 g mg^{-1} min^{-1} and K_2 (Mn) = 0.48 10^{-3} g mg^{-1} min^{-1}), with lower metal ions concentrations [54]. Due to the higher levels of heavy metals in DAM that in MIW, these facts showed that the process is probably dependent on the metal species content.

Initial adsorption rate of iron (h = 0.5 mg g^{-1} min^{-1}) was significantly higher than that of manganese (h = 0.091 mg g^{-1} min^{-1}), presumably influenced by pH values close to precipitation of Fe ions as hydroxides, in addition to the chemisorption phenomena. pH values for precipitation of Mn hydroxide (between 9 and 10) were not attained in the tested conditions. A higher sorption of metals onto the SS was observed in relation with different biosorbents, this being 1.38 mg Fe g^{-1} SS versus 0.15 mg Fe g^{-1} keratine [55], 0.35 mg Fe g^{-1} olive stone waste [56] and 0.65 mg Mn g^{-1} SS versus 0.36–0.41 mg Mn g^{-1} keratine [55]. Chitin polymer showed similar rates of sorption capacities for heavy metal removal when compared to SS [lead (up to 1.24 mg g^{-1}), cadmium (up to 1.81 mg g^{-1}), and cobalt (up to 0.93 mg g^{-1})] [57].

Conclusions

The experiments showed the significant effect of the biomaterial content on the remediation of AMD. Possibly, both the sorption process on the biomaterials and the influence of SS on the pH of the AMD to enhance the precipitation of metal hydroxides influence the removal of metals.

The effects of various experimental parameters on the AMD remediation were statistically investigated. By means of CCRD, an experimental program for modeling the effects of the agitation (X_1), MB content (X_2) and SS content (X_3) on metal removal (Fe and Mn) was designed.

Mathematical model equations were derived for the AMD removal by using the experimental data and the mathematical software package Statistica 13.1 *Statsoft*. A predictive model for Fe removal and Mn removal was established as a function of agitation for Fe and biomaterial contents (SS and MB) and agitation for Mn.

The adequacy of the predictive model was effectively verified by the validation data. It has been shown that the mathematical model CCRD (2^3) for Fe and Mn removal is valid by ANOVA at the 95% confidence interval. The predicted values were found to be in good agreement with the experimental values.

The optimum process parameters for the AMD remediation were determined to be: 136 rpm, 11.46 g L^{-1} SS and 71.6 g L^{-1} MB. The values of R^2 were close to 1, which indicated a high degree of correlation between the response and the independent variables for the two responses (experimental and predicted values).

The kinetic studies revealed that after a treatment time of 200 min, AMD was transformed in an effluent suitable for non-potable reuse with respect to the Fe and Mn contents. The pseudo-second-order model provided the best fitting of the experimental data, which confirmed that the process occurs via a chemical adsorption mechanism.

The sustainable nature of the proposed treatment should be noted. Highly contaminated water was transformed into water suitable for non-potable secondary use through the use of a low-cost technology that adds value to worthless wastes, i.e., SS and MB.

Acknowledgements The authors are grateful to the Department of Environmental Engineering at the Federal University of Santa Catarina (UFSC) and the Brazil and National Council of Scientific and Technologic Development (CNPq, CT-Mineral 51/2013) for financial and technical support. This paper is an extension of the work presented at the 4th International Conference on Energy and Environment Research – ICEER 2017 (Porto/Portugal) and published in Energy Procedia.

References

1. Johann, T., Martin, G., Sysman, M., Ina, G., Johann, S.: The 2012 acid mine drainage (AMD) crisis in Carolina's municipal water supply. Afr. Hist. Rev. **46**(2) 77–107 (2014). https://doi.org/10.1080/17532523.2014.943978
2. Valente, T., Grande, J., De La Torre, M., Gomes, P., Santisteban, M., Borrego, J., Braga, M.: Mineralogy and geochemistry of a clogged mining reservoir affected by historical acid mine drainage in an abandoned mining area. J. Geochem. Explor. **157**, 66–76 (2015). https://doi.org/10.1016/j.gexplo.2015.05.016
3. Sarmiento, A., Nieto, J., Cánovas, C., Olías, M.: La contaminación minera de los ríos Tinto y Odiel, Geología de la provincia de Huelva, pp. 173–183, (2016)
4. Trujillo, M.: Recuperación de suelos de relaves mineros para convertirlos en áreas verdes en la planta piloto metalúrgica de yauris-uncp. Convicciones **2**(1), 36–43 http://revistas.uncp.edu.pe/index.php/convicciones/article/viewFile/192/188 (2016). Accessed 14 Oct 2017
5. Amaral Filho, J., Schneider, I., De Brum, I., Sampaio, C., Miltzarek, G., Schneider, C.: Characterization of a coal tailing deposit for integrated mine waste management in the Brazilian coalfield of Santa Catarina. Revista Escola de Minas **66**(3), 347–353 (2013). https://doi.org/10.1590/S0370-44672013000300012
6. Soares, P., Castilhos, Z.: Recuperação de áreas degradadas pela mineração no Brasil, de IV Jornada do Programa de Capacitação Interna—CETEM, http://mineralis.cetem.gov.br/bitstream/cetem/1802/1/5%20-%20Pablo_Soares_JPCI_2015%20impresso.pdf (2015). Accessed 10 Sept 2017
7. Fávere, V., Laus, R., Laranjeira, M., Martins, A., Pedrosa, R.: Use of chitosan microspheres as remedial material for acidity and iron (III) contents of coal mining wastewaters. Environ. Technol. **25**, 861–866 (2004). https://doi.org/10.1080/09593330.2004.9619378
8. Manahan, S.E.: Environmental Chemistry, 10th edn., p. 752. CRC Press, Florida (2017)
9. Wilson, B., Pyatt, F.: Heavy metal dispersion, persistance, and bioccumulation around an ancient copper mine situated in Anglesey, UK. Ecotoxicol. Environ. Saf. **66**(2), 278–315, (2007). https://doi.org/10.1016/j.ecoenv.2006.02.015
10. Gazsó, L.G.: The key microbial processes in the removal of toxic metals and radionuclides from the environment. CEJOEM **7**(3–4), 178–185. http://www.omfi.hu/cejoem/Volume7/Vol7No3-4/CE01_3-4-03.html (2001). Accessed 9 Oct 2017
11. Kaksonen, A., Puhakka, J.: Sulfate reduction based bioprocesses for the treatment. Eng Life, **7**, 541–564, (2007). https://doi.org/10.1002/elsc.200720216
12. Robinson-Lora, M., Brennan, R.: Efficient metal removal and neutralization of acid mine drainage by crab-shell chitin under batch and continuous-flow conditions. Bioresour. Technol. **100**, 5063–5071, (2009). https://doi.org/10.1016/j.biortech.2008.11.063
13. Berghorn, G., Hunzekar, G.: Passive Treatment Alternatives for Remediation Abandoned Mine-Drainage. Wiley, New York (2001). https://doi.org/10.1002/rem.1007
14. Zipper, C., Skousen, J.: Acid Mine Drainage, Rock Drainage, and Acid Sulfate Soils: Causes, Assessment, Prediction, Prevention, and Remediation, pp. 339–353. Wiley, New York (2014)
15. Farooq, U., Kozinski, J., Khan, M., Athar, M.: Biosorption of heavy metal ions using wheat based biosorbents—a review of the recent literature. Bioresour. Technol. **101**, 5043–5053 (2010). https://doi.org/10.1016/j.biortech.2010.02.030
16. Liu, D., Zhu, Y., Li, Z., Tian, D., Chen, L., Chen, P.: Chitin nanofibrils for rapid and efficient removal of metal ions from water system. Carbohydr. Polym. **98**(1), 483–489 (2013). https://doi.org/10.1016/j.carbpol.2013.06.015
17. Anastopoulos, I., Bhatnagar, A., Bikiaris, D., Kyzas, G.: Chitin adsorbents for toxic metals: a review. Int. J. Mol. Sci. **18**(1), 114 (2017). https://doi.org/10.3390/ijms18010114
18. Mohameda, S., El-Gendya, A., Abdel-kader, A., El-Ashkar, E.: Removal of heavy metals from water by adsorption on chitin derivatives. Der Pharm. Chem. **7**(10), 275–283. http://www.derpharmachemica.com/pharma-chemica/removal-of-heavy-metals-from-water-by-adsorption-on-chitin-derivatives.pdf (2015). Accessed 30 Aug 2017
19. Rhazi, M., Desbrières, J., Tolaimate, A., Rinaudo, M., Vottero, P., Alagui, A., Meray, M.: Influence of the nature of the metal ions on the complexation with chitosan.: application to the treatment of liquid waste. Eur. Polym. J. **38**(8), 1523–1530 (2002). https://doi.org/10.1016/S0014-3057(02)00026-5
20. Bassi, R., Prasher, S., Simpson, B.: Effects of organic acids on the adsorption of heavy metal ions by chitosan flakes. J. Environ. Sci. Health. **34**(2), 289–294 (1999). https://doi.org/10.1080/10934529909376836
21. Pradhan, S., Shukla, S., Dorris, K.: Removal of nickel from aqueous solutions using crab shells. J. Hazard. Mater. **125**(1–3), 201–204 (2005). https://doi.org/10.1016/j.jhazmat.2005.05.029
22. Xu, Y., Gallert, C., Winter, J.: Chitin purification from shrimp wastes by microbial deproteination and decalcification. Appl. Microbiol. Biotechnol. **79**(4), 687–697 (2008). https://doi.org/10.1007/s00253-008-1471-9
23. Das, S., Roy, D., Sen, R.: Utilization of chitinaceous wastes for the production of chitinase. Adv. Food Nutr. Res. **78**, 27–46 (2016). https://doi.org/10.1016/bs.afnr.2016.04.001
24. Bajaj, M., Freiberg, A., Xu, W.J., Gallert, Y.: C.: Pilot-scale chitin extraction from shrimp shell waste by deproteination and decalcification with bacterial enrichment cultures. Appl. Microbiol. Biotechnol. **99**(22), 9835–9846 (2015). https://doi.org/10.1007/s00253-015-6841-5 no.
25. Rinaudo, M.: Chitin and chitosan: properties and applications. Prog. Polym. Sci. **31**(7), 603–632, (2006). https://doi.org/10.1016/j.progpolymsci.2006.06.001
26. Qu, T., Verma, D., Alucozai, M., Tomar, V.: Influence of interfacial interactions on deformation mechanism and interface viscosity in α-chitin–calcite interfaces. Acta Biomater. **25**, 325–338 (2015). https://doi.org/10.1016/j.actbio.2015.06.034
27. Núñez-Gómez, D., Nagel-Hassemer, M.E., Lapolli, F., Lobo-Recio, M.A.: Potential of shrimp-shell residue in natura for the remediation of mine impacted water (MIW). Polímeros, **26**, 1–7 (2016). https://doi.org/10.1016/j.egypro.2017.10.248
28. Núñez-Gómez, D., Aparecida, A., Nagel-Hassemer, M.E., Lapolli, F., Lobo-Recio, M.A.: Aplication of the statistical experimental design to optimize mine-impacted water (MIW) remediation using shrimp-shell. Chemosphere, **167**, 322–329 (2017). https://doi.org/10.1016/j.chemosphere.2016.09.094
29. USEPA—United States Environmental ProtectionAgency: Method 3005A: Acid Digestion of Waters for Recoverable or Dissolved Metals for Analysis by FLAA or ICP Spectroscopy. USEPA—United States Environmental ProtectionAgency Washington DC (1992)
30. USEPA—United States Environmental ProtectionAgency: Method 3010A: Acid Digestion of Aqueous Samples and Extracts for Total

Metals for Analysis by FLAA or ICP Spectroscopy. USEPA—United States Environmental ProtectionAgency Washington DC (1992)
31. APHA—American Public Health Association: «3110 Metals by Atomic Absorption Spectrometry,» de Standard Methods for the Examination of Water and Wastewater, 22nd edn. APHA—American Public Health Association, Washington DC (2016)
32. Box, G., Hunter, W., Hunter, S.: An Introduction to Design, Data Analysis, and Model Building, Statistics for Experimenters, pp. 374–434. Wiley, New York (1978)
33. Lagergren, S.: About the theory of so-called adsorption of soluble substances. Kungliga Svenska Vetenskapsakademiens Handlingar **24**, 1–39 (1898)
34. Porter, J., McKay, G.: The prediction of sorption from a binary mixture of acidic dyes using single- and mixed isotherm variants of the ideal adsorbed solute theory. Chem. Eng. Sci. **54**, 5863–5885 (1999). https://doi.org/10.1016/S0009-2509(99)00178-5
35. Morris, J.,. Weber, J.: Kinetics of adsorption on carbon from solution. ASCE **89**(SA2), 31–59 (1963)
36. Low, K., Lee, C., Liew, S.: Sorption of cadmium and lead from aqueous solutions by spent grain. Process Biochem. **36**(1–2), 59–64 (2000). https://doi.org/10.1016/S0032-9592(00)00177-1
37. Tütem, E., Apak, R., Unal, C.: Adsorptive removal of chlorophenols from water by bituminous shale. Water Res. **32**, 2315–2324, (1998). https://doi.org/10.1016/S0043-1354(97)00476-4
38. Daubert, L., Brennan, R.: Passive remediation of acid mine drainage using crab shell chitin. Environ. Eng. Sci. **24**(10), 1475–1480 (2007). https://doi.org/10.1089/ees.2006.0199
39. Subhabrata, D., Shantonu, R., Jayanta, B.: Optimization of the operation of packed bed bioreactor to improve the sulfate and metal removal from acid mine drainage. J. Environ. Manage. **200**, 135–144, (2017). https://doi.org/10.1016/j.jenvman.2017.04.102
40. Skousen, J., Zipper, C., Ziemkiewicz, P., Nairn, R., McDonald, L., Kleinmann, R.L.: Review of passive systems for acid mine drainage treatment. Mine Water Environ. **36**(1), 133–153, (2017). https://doi.org/10.1007/s10230-016-0417-1
41. Brazil, National Environment Council—Resolução CONAMA 430/2011. Provisions the conditions and standards of effluents and complements and changes Resolution 357 from March 17, 2005 issued by the National Environment Council (CONAMA), (2011)
42. Brasil, J., Ev, R., Milcharek, C., Martins, L., Pavan, F.: Statistical design of experiments as a tool for optimizing the batch conditions to Cr(VI) biosorption on Araucaria angustifolia waste. J. Hazard. Mater. **B133**, 143–153 (2006). https://doi.org/10.1016/j.jhazmat.2005.10.002
43. Saramago, S., Silva, N.: Uma introdução ao estudo de superfícies de resposta, de Revista Horizonte Científico, 4a edn., Universidade Federal de Uberlândia, Uberlândia (2005)
44. Gerente, C., Lee, V., Le Cloirec, P., McKay, G.: Application of chitosan for the removal of metals from wastewaters by adsorption-mechanisms and models review. Rev. Environ. Sci. Bio/Technol. **37**, 41–127 (2007). https://doi.org/10.1080/10643380600729089
45. Degremont, W.: Treatment Handbook, pp. 1211–1216. Degremont, Paris (1991)
46. Robinson-Lora, M., Brennan, R.: Biosorption of manganese onto chitin and associated proteins during the treatment of mine impacted water. Chem. Eng. J. **162**, 565–572 (2010). https://doi.org/10.1016/j.cej.2010.05.063
47. Brazil, National Environment Council - Resolução CONAMA 357/2005. Establishes provisions for the classification of water bodies as well as environmental directives for their framework, establishes conditions and standards for effluent releases and makes other provisions, (2005)
48. Ong, S., Seng, C., Lim, P.: Kinetics of adsorption of Cu (II) and Cd (II) from aqueous solution on husk and modified rice husk. Electron. J. Environ. Agric. Food Chem. **6**(2), 1764–1774, (2007)
49. Ho, Y., McKay, G.: The kinetics of sorption of divalent metal ions onto sphagnum moss peat. Water Res. **34**, 735–742 (2000). https://doi.org/10.1016/S0043-1354(99)00232-8 nº 3
50. Wu, F., Tseng, R., Juang, R.: Characteristics of Elovich equation used for the analysis of adsorption kinetics in dye-chitosan systems. Chem. Eng. J. **150**, 366–373 (2009). https://doi.org/10.1016/j.cej.2009.01.014 nº 2
51. Taylor, R., Hassan, K., Mehadi, A., Shuford, J.: Kinetics of zinc sorption by soils. Commun. Soil Sci. Plant Anal. **26**(11–12), 1761–1771 (1995). https://doi.org/10.1080/00103629509369407
52. Siu, P., Koong, L., Saleem, J., Barford, J., McKay, G.: Equilibrium and kinetics of copper ions removal from wastewater by ion exchange. Chin. J. of Chem. Eng. **24**, 94–100 (2016). https://doi.org/10.1016/j.cjche.2015.06.017 nº 1
53. Ho, Y., McKay, G.: Kinetics of pollutant sorption by biosorbents: review. Sep. Purif. Rev. **29**(2), 189–232 (2000). https://doi.org/10.1081/SPM-100100009
54. Nuñez-Gómez, D.. Potencial da casca de camarão para remediação de águas contaminadas com drenagem ácida mineral visando seu reuso secundário não potável. Master These. Federal University os Santa catarina—Brazil, (2014)
55. Ramírez-Paredes, F.I., Manzano-Muñoz, T., Garcia-Prieto, J.C., Bello-Estévez, J.F., Zhadan, G.G., Shnyrov, V.L., Roig, M.G.: Biosorption of heavy metals from acid mine drainages onto pig bristles, poultry feathers and crustacean shells industrial biowastes. J. Basic Appl. Sci. **9**, 510 (2013). https://doi.org/10.6000/1927-5129.2013.09.66
56. Hodaifa, G., Ochando-Pulido, J.M., Alami, S.B.D., Rodriguez-Vives, S., Martinez-Ferez, A.: Kinetic and thermodynamic parameters of iron adsorption onto olive stones. Ind. Crops Prod. **49**, 526–534 (2013). https://doi.org/10.1016/j.indcrop.2013.05.039
57. Pinto, P.X., Al-Abed, S.R., Reisman, D.J.: Biosorption of heavy metals from mining influenced water onto chitin products. Chem. Engineering J. **166**(3), 1002–1009 (2011). https://doi.org/10.1016/j.cej.2010.11.091

Affiliations

Dámaris Núñez-Gómez[1] · Flávio Rubens Lapolli[1] · Maria Elisa Nagel-Hassemer[1] · María Ángeles Lobo-Recio[1,2]

✉ María Ángeles Lobo-Recio
maria.lobo@ufsc.br

[1] Department of Environmental Engineering, Federal University of Santa Catarina (UFSC), P. O. Box 476, Florianópolis 88040-970, SC, Brazil

[2] Department of Energy and Sustainability, Federal University of Santa Catarina (UFSC), Rodovia Jorge Lacerda 3201, Araranguá 88900-000, SC, Brazil